Fusion Engineering and Design 123 (2017) 950–954

Contents lists available at ScienceDirect

Fusion Engineering and Design

journal homepage: www.elsevier.com/locate/fusengdes

Automatic ELM detection using gSPRT on the COMPASS tokamak

M. Berta[a,*], M. Szutyányi[a], A. Bencze[b], M. Hron[c], R. Pánek[c]

[a] Széchenyi István University, Győr, Hungary
[b] Wigner RCP, HAS, Budapest, Hungary
[c] Institute of Plasma Physics AS CR, Prague, Czech Republic

HIGHLIGHTS

- The gSPRT method automatically detects ELMs in D_α and also in Mirnov signals.
- ADFs of conditionally averaged ELM effect in D_α and Mirnov signals has been determined.
- The gSPRT method has been compared with two other techniques and seems to be more realistic.
- Average radial propagation velocity of ELMs has been determined as ~1 km/s.

ARTICLE INFO

Article history:
Received 3 October 2016
Received in revised form 13 February 2017
Accepted 6 March 2017
Available online 21 March 2017

Keywords:
ELM
Plasma diagnostics
COMPASS tokamak
Automatic detection
GSPRT

ABSTRACT

This paper contains the description of the generalized Sequential Probability Ratio Test (gSPRT) method used for automatic ELM detection in different diagnostic signals collected on the COMPASS tokamak. After determination of H-mode region based on D_α signal in a given shot, ELMs are automatically detected in different diagnostic time traces (e.g. magnetic signals and also in D_α signals). The onset time, the maximum location and the peak value, and the duration of each detected ELM is determined. Analyzed diagnostic signals came from different radial positions of the studied plasma volume, thus from arrival times of given ELM into different detectors, the average radial propagation velocity of the ELM event can be also estimated. Comparison of results from gSPRT method with two different, commonly used automatic ELM detection method (threshold technique and correlation based technique) is also reported.

1. Introduction

Edge Localized Modes (ELMs) are quasi-periodic events occurring at the edge of fusion plasmas in high confinement mode (H-mode), and releasing significant part of energy and particles confined in the plasma. Released energy and particles arrive on the first wall of the fusion device and represent extreme heat load for the components of the first wall [1–3].

Extreme heat loads on the first wall of energetic fusion reactors, such as ITER and DEMO, are not acceptable. Thus the understanding of physics governing ELM events is the key issue for operation of energetic fusion reactors. That is why ELMs are intensively studied on every existing fusion device capable of ELMy H-mode operation including the COMPASS tokamak [4].

The effect of ELM events on diagnostic signals is clearly observable by eye, but for the massive experimental data analysis automatic ELM detection technique is necessary [5,6]. We report in this paper a generalized statistical method, called *generalized Sequential Probability Ratio Test (gSPRT)* for automatic ELM detection.

2. The SPRT method and it's generalization to gSPRT

The classical Sequential Probability Ratio Test (SPRT) was published in 1945 as a statistical tool in the quality control industry in order to *distinguish between two random processes (P_1 and P_2) in a measurement* [7]. The key element of this method is the *logarithmic probability ratio* defined as:

$$\lambda_n = \ln \frac{p_1(z_1, z_2, \ldots, z_n|\mu_1, \sigma_1)}{p_2(z_1, z_2, \ldots, z_n|\mu_2, \sigma_2)}, \quad (1)$$

where $p_1(z_1, z_2, \ldots, z_n|\mu_1, \sigma_1)$ – is the cumulative probability, that time sequence $z_1, z_2, \ldots, z_n$ belongs to process P_1 characterized by p_1 probability density function with parameters μ_1 and σ_1, $p_2(z_1, z_2, \ldots, z_n|\mu_2, \sigma_2)$ – is the cumulative probability, that time sequence

* Corresponding author.
E-mail address: bertam@sze.hu (M. Berta).

http://dx.doi.org/10.1016/j.fusengdes.2017.03.025
0920-3796/

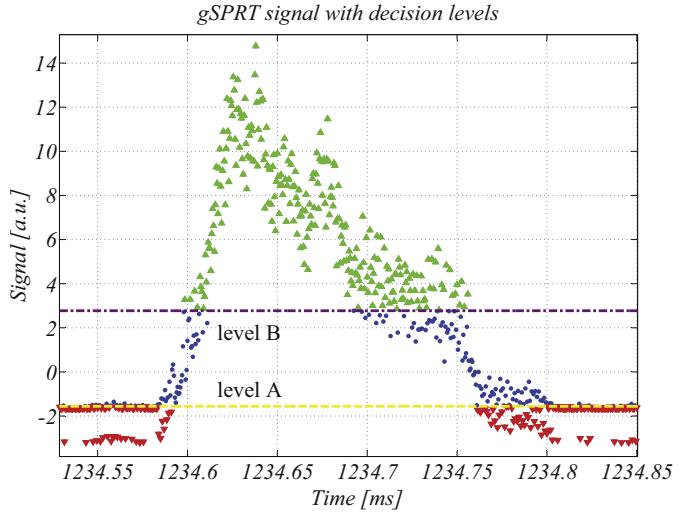

Fig. 1. The decision procedure of SPRT shown on the measured D_α signal.

$z_1, z_2, \ldots, z_n$ belongs to process P_2 characterized by p_2 probability density function with parameters μ_2 and σ_2.

In order to be able to decide on the basis of logarithmic probability ratio, that is, if some sample z_n belongs to P_1 or to P_2 process we need to define decision levels. Decision levels in SPRT method are defined using two prescribed probabilities:

- α – *the probability of "false alarm"* – probability that sample z_n belongs to process P_1 even it is not the case.
- β – *the probability of "missed alarm"* – probability that sample z_n does not belong to process P_1 even it is the case.

Using the probabilities α and β, the decision levels are defined as:

$$A = \ln \frac{\beta}{1-\alpha}, \quad B = \ln \frac{1-\beta}{\alpha},$$

and the decision procedure is as follows:

- If $\lambda_n < A$ – signal sample "belongs" to process P_2. After this decision SPRT sets-up $\lambda_n = 0$ (see ▼ in Fig. 1).
- If $\lambda_n > B$ – signal sample belongs to process P_1. After this decision SPRT sets-up $\lambda_n = 0$ (see ▲ in Fig. 1).
- If λ_n is between decision levels SPRT will not make any decision, and the test will go on with the next sample (see ● in Fig. 1).

Generalization of the classical SPRT for non-stochastic processes proposed in the present work can be done in three steps:

- In the logarithmic probability ratio we use fitted empirical amplitude distribution functions (ADF) instead of probability density functions (PDF) of stochastic processes ([8,9]). As the ADF can be defined for deterministic processes as well, this step gives the *possibility to use the method for non-stochastic processes*.
- Data samples recorded during the ELM events are considered as parts of the process P_1, while the samples of the inter-ELM periods belong to the process P_2.
- According to the experiments [4] the ELM duration is restricted to $\tau_{ELM} = [100, 300]$ μs.

3. Empirical amplitude distribution functions of ELM events

Systematic investigations of diagnostic signals have shown that the ADF of the inter-ELM periods (process P_2) in both signals can

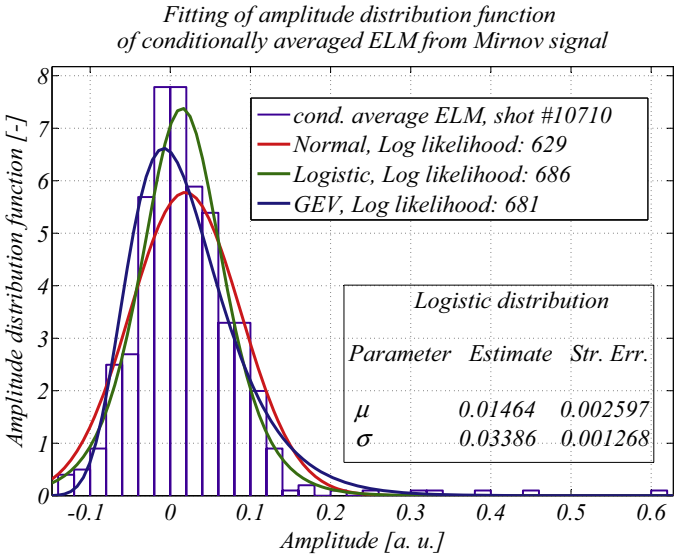

Fig. 2. Fitting of different distribution functions to conditionally averaged Mirnov signal ADF data.

be well described by the Gaussian distribution (2). We have also found that the mean value (μ_0) and the standard deviation (σ_0) of this normal distribution is constant during the whole H-mode after filtering and detrending both the Mirnov signal and the D_α signal.

$$\rho_{Gauss}(z; \mu_0, \sigma_0) = \frac{1}{\sqrt{2\pi}\sigma_0} \exp\left(-\frac{(z-\mu_0)^2}{2\sigma_0^2}\right) \tag{2}$$

3.1. ADFs for process P_1 in Mirnov signals

For Mirnov signals we have concluded in each case (in every shot) that the best fit for the empirical ADF for conditionally averaged ELM effect [10] is the Logistic distribution (3) (Fig. 2).

$$\rho_{Logistic}(z; \mu, \sigma) = \frac{\exp\left(\frac{z-\mu}{\sigma}\right)}{\sigma\left(1+\exp\left(\frac{z-\mu}{\sigma}\right)\right)^2} \tag{3}$$

Mirnov coil signals are "double sided" (both negative and positive values are present). Calculations show that it is a good approximation that we set the μ_0 of the process P_2 and μ of process P_1 to zero.

3.2. ADFs for process P_1 in D_α signals

For D_α signals we have found very interesting competitive situation. In most of the cases (in most of the shots) the best fit for the empirical ADF for conditionally averaged ELM [10] was the Wald (also known as Inverse Gauss) distribution (4), but in a significant number of cases the Generalized Extreme Value (GEV) distribution turned out to be the best fit. In all cases however we have found the difference in "goodness" for these two competitive distributions small. Finally we decided to use as the "best fit" of ADFs for process P_1 in D_α signals the Wald distribution. The reason for this choice was the fewer number of free parameters for the Wald distribution, namely (μ, Λ). Detailed investigations has shown that the shape parameter (Λ) has small standard deviation ~0.5 in each considered plasma discharge (Fig. 3).

$$\rho_{Wald}(z; \mu, \Lambda) = \sqrt{\frac{\Lambda}{2\pi z^3}} \exp\left(-\frac{\Lambda(z-\mu)^2}{2\mu^2 z}\right) \tag{4}$$

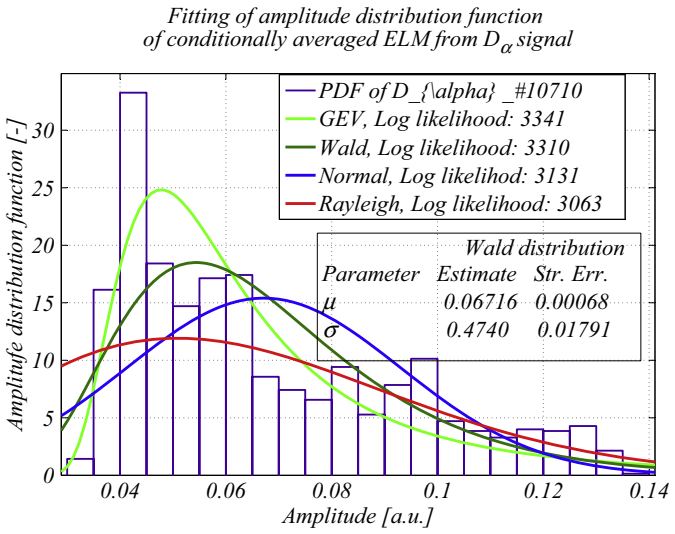

Fig. 3. Fitting of different distribution functions to conditionally averaged D_α signal's ADF.

Using the above defined distributions, the gSPRT signal can be calculated recursively as follows:

$$\lambda_1^{Mirnov} = 0 \quad \lambda_1^{D_\alpha} = 0$$

From (2) and (3), we obtain the following recursive expression for λ_{n+1}^{Mirnov}:

$$\lambda_{n+1}^{Mirnov} = \lambda_n^{Mirnov} + \ln \frac{\rho_{Logistic}(z_{n+1}; \mu, \sigma)}{\rho_{Gauss}(z_{n+1}; \mu_0, \sigma_0)} \tag{5}$$

From (2) and (4), we obtain the following recursive expression for $\lambda_{n+1}^{D_\alpha}$:

$$\lambda_{n+1}^{D_\alpha} = \lambda_n^{D_\alpha} + \ln \frac{\rho_{Wald}(z_{n+1}; \mu, \Lambda)}{\rho_{Gauss}(z_{n+1}; \mu_0, \sigma_0)} \tag{6}$$

4. gSPRT results for different diagnostic signals

Let us now use the algorithm described above for Mirnov and D_α signals recorded during COMPASS ELMy H-mode discharges. We set $\alpha = 0.2$ and $\beta = 0.05$. We note that the gSPRT method is not sensitive to small variations of these values. In the majority of cases the H-mode times are stored in the COMPASS database (CDB), and we have used these data in our analysis, there are however a few cases where we have determined the H-mode times directly from D_α signals (Fig. 4).

In order to demonstrate the usage of the gSPRT we have chosen two data channels from different diagnostics, namely an edge D_α channel and a midplane Mirnov-coil. The further analysis has been done for parts of the signals collected during H-mode. The gSPRT algorithm has been implemented in the following steps:

1 Prior to the application of gSPRT the measured diagnostic signals need to be cleared from uncorrelated noise. For this purpose we use optimal Golay–Savitzky filters. The optimal orders of these filters have been chosen on the basis of *Akaike information criterion* ([11]).
2 The average level of D_α signal inbetween ELMs linearly increases, because of better confinement of impurities during H-mode. This increase is removed from D_α signals using linear detrending algorithm. In case of magnetic signals this increase is not present, thus the usage of detrending is not necessary (mean value of Mirnov signals is near to zero).

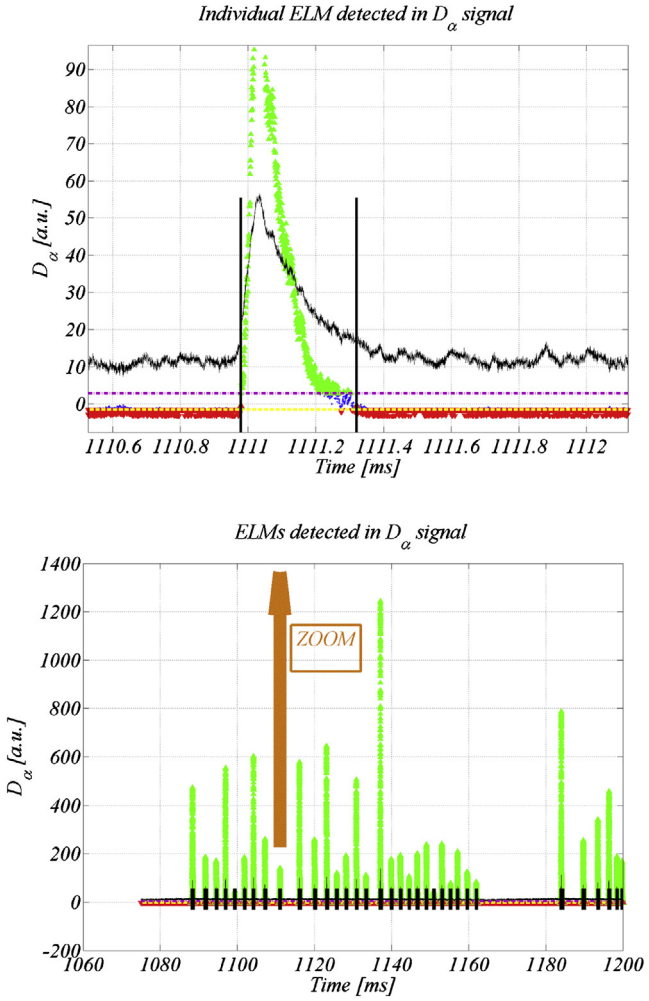

Fig. 4. The gSPRT signal for measured D_α signal in the shot #11733 (bottom) and the zoomed view for one ELM event (top).

3 A small part of the signal has been chosen from a time range "assumed" to be between two consecutive ELMs. The root mean square (σ_p) of this signal segment has been calculated, and the self-check has been made:
   - For Mirnov signals: μ and μ_0 from (3) and (2) have been set to zero. σ from (3) has been set as $4\sigma_p$, and σ_0 from (2) has been set as $2\sigma_p$. (We have to note that the coefficient 4 for σ and 2 for σ_0 can be chosen from a relatively wide range of values without significant effect on the results.) The gSPRT signal has been calculated by means of (5) using these parameters.
   - For D_α signals: the μ_0 parameter in (2) has been set to the mean signal level (M) of the H-mode data, and the σ_0 to $2\sigma_p$. The μ parameter of expression (4) has been set to $1.5M$, and the shape parameter (Λ) to 0.5. The gSPRT signal has been calculated using (6).
   - If the whole gSPRT signal is under the B decision level (there is no ▲ symbol in the gSPRT signal) we have chosen an inter-ELM segment, if this is not the case, the algorithm chooses another small part of the signal and re-checks it.
4 We have calculated the gSPRT signal for the whole region of H-mode, and the algorithm detects the ELM events automatically on the base of gSPRT signal. To determine ELM occurrence and ELM duration we have scanned the gSPRT signal with the moving time window of given length T_{sc} (we are using $T_{sc} = 25\,\mu s$ corresponding to 50 samples).

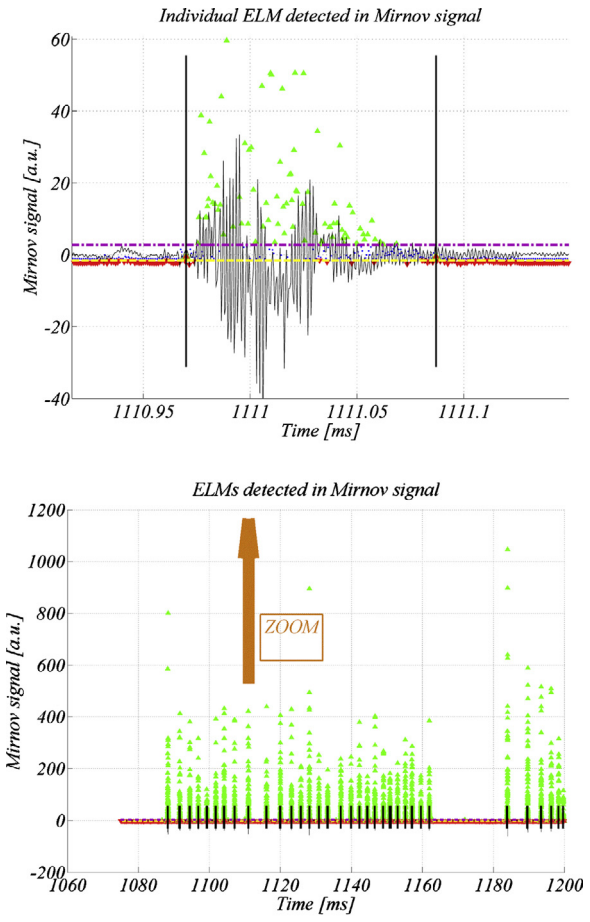

Fig. 5. The gSPRT signal for measured Mirnov signal in the shot #11733 (bottom) and the zoomed view for one ELM event (top).

When the gSPRT signal crosses the decision level B a time interval of dominance I_i opens. If at least one gSPRT value is above the decision level B during the next scan step the time interval I_i will remain opened. If in one consecutive scan step all values of gSPRT signal are below the decision level B, the time interval I_i will be closed with the last time point, when value of gSPRT was above the decision level B. From the definition of decision level B is clear, during the time interval I_i the analyzed signal is dominated by the ELM process.

To determine the duration of each ELM we have to extend intervals of dominance I_i for each ELM. We have added time interval $I_i^{(b)}$ before interval I_i, respectively time interval $I_i^{(a)}$ after interval I_i. For each time interval we have defined the ratio (R) of number of time points with gSPRT values below the decision level A to the number of time points with gSPRT values above the decision level A. Lengths of additional intervals have been chosen in order to set rates $R^{(b)}$ respectively $R^{(a)}$ in each additional interval equal to $0.9 \times R^0$. The ratio $R^{(0)}$ has been calculated for inter-ELM segment determined in the 3. step. (the gSPRT signal for D_α trace can be seen in Fig. 4 and for Mirnov-coil data in Fig. 5.)

5 All events detected accordingly to the set false alarm rate, which are shorter than 100 μs or longer than 300 μs have not been classified as ELM and have been filtered out.

5. Comparison of the gSPRT with other methods

In order to asses the relevance of the gSPRT method it has been compared with two other techniques used for automatic ELM detection. The first is the threshold method ([12]) and the second

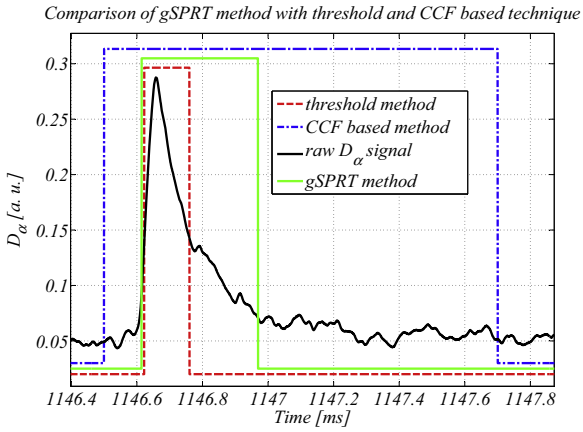

Fig. 6. Comparison of three automatic ELM detection methods.

is the Cross-Correlation Function (CCF) based method ([13]), which is commonly used on the COMPASS tokamak.

In the shot #11733 the start of ELMs in D_α signal has been detected 7 μs earlier (in average) by the gSPRT than by the threshold method. On the other hand the end time of ELMs in D_α signal was detected 198 μs later (in average) by the gSPRT compared to the threshold method.

Although the CCF based method detected the start of ELMs earlier, and the end of ELMs later than the gSPRT, from Fig. 6 is clear that these time points do not belong to the ELM event, rather they seem to belong to the process going on between ELMs. We note that all three compared methods have been automatically detected the same number of ELMs at the same locations, but gSPRT seems to be more reliable and precise.

6. Estimation of average ELM propagation radial velocity

It is widely accepted in the literature that the ELMs are results of peeling-balooning instability, thus the process starts with increasing magnetic perturbations. These magnetic perturbations are seen in Mirnov coil signals. Energy and particles released by ELM events are moving towards to first wall. D_α detectors can detect the effect of released and recycled (recombined at the wall) particles radiating in the plasma edge. The time delay between magnetic and D_α detectors allow us to determine a lower limit for radial propagation velocity of the ELM crash, if we know the space separation of detectors. The propagation time was estimated as the delay of ELM start detected by Mirnov detector and D_α detector and it's average value during H-mode in shot #11733 was $\Delta\tau \sim 20$ μs. We should emphasize again that the propagation time includes the time needed for the recycling of hot plasma particles. The gap between the separatrix and first wall on the COMPASS tokamak in shot #11733 can be estimated from EFIT reconstruction, and during whole H-mode it was almost constantly $\Delta s \sim 2$ cm (Fig. 7).

The lower limit for average radial propagation velocity of ELMs in shot #11733 can be estimated as:

$$\tilde{v}_r \sim \frac{\Delta s}{\Delta \tau} \sim 1\ \mathrm{km/s} \tag{7}$$

7. Conclusions

In the present contribution we have suggested and demonstrated a generalization of the SPRT method for robust and accurate automatic ELM detection in fusion plasmas. The gSPRT method reliably finds ELMs automatically in diagnostic signals measured on the COMPASS tokamak based on empirical properties of measured signals. The gSPRT detects the start time of ELMs slightly

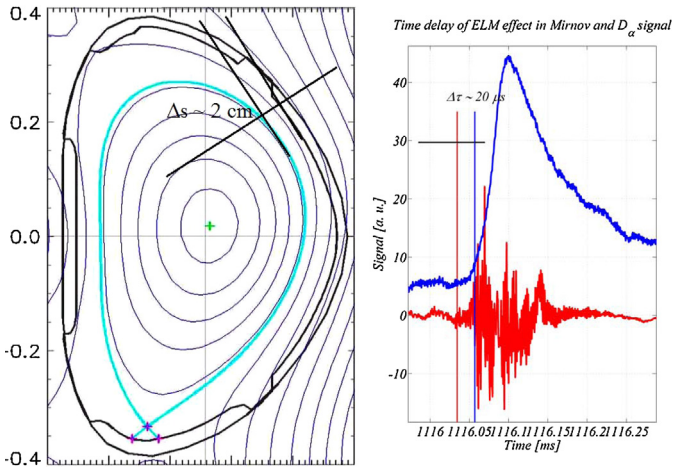

Fig. 7. ELM's average propagation velocity estimation in shot #11733.

earlier and the end of ELMs significantly later than the threshold method. An average time delay of ~20 μs has been observed between appearences of ELMs' effects in Mirnov and D_α signals suggesting an average propagation faster than ~1 km/s.

Acknowledgements

The work was partly supported by project "Support of Széchenyi István University in innovation" financed by Hungarian Government (identification number: 1687/2015. (IX. 25.)), partly supported by Czech Science Foundation project GA16-25074S and co-funded by MEYS projects 8D15001 and LM2015045.

References

[1] H. Zohm, Plasma Phys. Control. Fusion 38 (1996) 105–128.
[2] J.W. Connor, Plasma Phys. Control. Fusion 40 (1998) 531–542.
[3] A. Kirk, et al., Phys. Rev. Lett. 92 (2004) 245002.
[4] R. Pánek, et al., Plasma Phys. Control. Fusion 58 (2015), 014015 (9pp).
[5] S. González, et al., Fusion Sci. Technol. 58 (2010) 755–762.
[6] M. Lennholm, et al., Nucl. Fusion 55 (2015) 063004, http://dx.doi.org/10.1088/0029-5515/55/6/063004.
[7] A. Wald, Sequential tests of statistical hypotheses, Ann. Math. Stat. 16 (2) (1945) 117–186, http://dx.doi.org/10.1214/aoms/1177731118.
[8] G. Szappanos, G. Por, Improvements in the theory of identification of burst-shaped events for fault diagnosis, Nucl. Sci. Eng. 130 (1998) 261–267.
[9] M. Berta, G. Por, The rolling motion of the core barrel in WWER 440 type reactors, in: Proceedings of IMORN 28, Athens, 2000.
[10] T. Huld, A.H. Nielsen, H. Pécseli, J. Juul Rasmussen, Phys. Fluids B 3 (1991) 1609, http://dx.doi.org/10.1063/1.859680.
[11] H. Akaike, A new look at the statistical model identification, IEEE Trans. Automat. Control 19 (6) (1974), http://dx.doi.org/10.1109/TAC.1974.1100705.
[12] R.A. Pitts, et al., On the statistics of ELM filaments measured by fast low field side wall Langmuir probes on TCV, in: 34th EPS Conference on Plasma Phys., Warsaw, 2–6 July 2007 ECA Vol.31F, P-2.026, 2007.
[13] L. Di Stefano, et al., ZNCC – based template matching using bounded partial correlation, Pattern Recognit. Lett. 26 (2005) 2129–2134.